Mineralogy and Petrology
https://doi.org/10.1007/s00710-024-00871-4

RESEARCH

Unveiling CCS Potential of the Rio Bonito Formation, Paraná Basin, southern Brazil: The Dawsonite Discovery

Letícia L. Mallmann[1] · Augusto G. Nobre[2] · Farid Chemale Jr[1] · Renata G. Netto[1] · Paulo Sérgio G. Paim[1] · Rita Fabiane G. de Oliveira[1]

Received: 20 April 2024 / Accepted: 20 August 2024

Abstract
Dawsonite, a hydrated carbonate, is a key mineral studied for Carbon Capture and Storage (CCS) initiatives. It forms in high pCO_2 environments, enabling gas storage in a solid state within geological reservoirs, thereby helping mitigate greenhouse gas emissions. The Rio Bonito Formation has gained attention as a potential CO_2 reservoir due to its favorable characteristics such as porosity, permeability, depth, thickness, organic matter content, and the presence of an effective sealing layer (Palermo Formation), particularly in the central region of the Paraná Basin. This study reveals the natural occurrence of dawsonite within the Rio Bonito Formation in the southern part of the Paraná Basin, in Rio Grande do Sul State, Brazil. Dawsonite was identified in quartz sandstones through petrographic analysis, indicating its formation during mesodiagenesis, where it crystallized within moldic pores. The presence of dawsonite was further confirmed through scanning electron microscopy coupled with energy-dispersive X-ray spectroscopy (SEM–EDX) and X-ray diffraction (XRD) techniques. This discovery marks the first documented occurrence of dawsonite within the Rio Bonito Formation. It suggests that under similar conditions, other sections of the Rio Bonito Formation may also include dawsonite, thereby expanding the potential for onshore CCS in the Paraná Basin.

Keywords Mineral trapping · Carbon sink minerals · Carbonate crystallization · Carbon neutrality · CO_2 injection

Introduction

Dawsonite, a hydrated sodium aluminum carbonate ($NaAlCO_3(OH)_2$), was considered a rare mineral up to the twentieth century (Loughnan and Goldbery 1972). However, today it is regarded as an unusual mineral on Earth's surface, having been identified in several parts of the world. Examples include Argentina (Comerio et al. 2014), Australia (Golab et al. 2006), Belarus (Limantseva et al. 2008), Brazil (Teles et al. 2022), China (Liu et al. 2011; Li et al. 2024), Italy (Wopner and Höcker 1987), Japan (Okuyama 2014), Mongolia (Dong et al. 2011), Poland (Rybak-Ostrowska et al. 2020), Romania (Cseresznyes et al. 2024), Tanzania (Hay and Reeder 1991), United States (Burnham et al. 2015), and Yemen (Worden 2006). Dawsonite belongs to the orthorhombic crystal system and was first identified by Harrington (1875). It is a whitish mineral with a silky luster and a fine fibrous habit (Golab et al. 2006), occurring mainly in an authigenic subsurface context. It is substantially more unstable and therefore rarer on the surface (Saldanha et al. 2023; Cseresznyes et al. 2024).

Mineral dawsonite forms at temperatures between 25 and 200 ºC (Li et al. 2017; Qu et al. 2022), while synthetic dawsonite can be produced between 60 and 180 ºC (Li et al. 2022; Knorpp et al. 2023) under high partial pressure of CO_2 (Marinos et al. 2021; Li et al. 2023) and remains stable in alkaline pH environments (Hellevang et al. 2010). Dawsonite is mostly found in rocks at depths between 1000 and 2200 m (Qu et al. 2022), although there are records of its occurrence at depths shallower than 200 m (Limantseva et al. 2008; Comerio et al. 2014 and this work) and at depths

Editorial handling: F. Lucci

✉ Augusto G. Nobre
augusto.nobre@ufsm.br

[1] Escola Politécnica, Universidade do Vale do Rio dos Sinos, Av. Unisinos, 950 - Cristo Rei, São Leopoldo, Rio Grande do Sul 93022-750, Brazil

[2] Departamento de Geociências, Universidade Federal de Santa Maria, Av. Roraima, 1000 - Prédio 17 - Camobi, Santa Maria 97105-000, Brazil

Published online: 06 September 2024

greater than 3000 m (Worden 2006). It is mainly found in clastic rocks, accounting for approximately 75% of its occurrence (Qu et al. 2022), including feldspathic (Li and Li 2016) and quartz sandstones (Gao et al. 2009), pyroclastic rocks (Dong et al. 2011) and sedimentary tuffs (Zalba et al. 2011). Dawsonite is also recorded in igneous rocks (Sirbescu and Nabelek 2003), limestones (Goldbery and Loughnan 1977), oil shales (Palayangoda and Nguyen 2015), coal (Ming et al. 2017) and soils (Reynolds et al. 2012).

Dawsonite has recently gained prominence due to its CO_2 mineral trapping potential (Hellevang et al. 2005, 2011, 2013; Kaszuba et al. 2011; Lu et al. 2022). Initiatives to mitigate greenhouse gas (GHG) atmospheric concentrations by safely storing GHGs in the subsurface for long periods (Carbon Capture and Storage—CCS) have been gaining notoriety as carbon neutrality and circular economy policies become popular (Nobre et al. 2021, 2022a). Mineral trapping is a type of CCS strategy discussed since the 1990s (Lohuis 1993), involving the injection of CO_2 into geological reservoirs with suitable compositions, porosities, permeabilities, fluids, and thermodynamic conditions to cause the precipitation of carbonate mineral phases (e.g., dawsonite), thereby immobilizing the CO_2 in the formation (Bachu et al. 1994). Geochemical (Gaus et al. 2005) and CO_2 injection models (Johnson et al. 2004) for mineral trapping with dawsonite crystallization have demonstrated higher potential for long-lasting CCS than strategies such as hydrodynamic or dissolution capture (Moore et al. 2005). However, if pCO_2 in the formation is not kept high, dawsonite can destabilize and release CO_2 (Hellevang et al. 2005; Ketzer et al. 2005; Lu et al. 2022). This indicates that the rock package must meet specific prerequisites to behave as an effective CO_2 reservoir.

A good geological reservoir for mineral trapping must present a permeability high enough to allow the mobility and dissemination of CO_2 in the subsurface, in addition to high porosity to accommodate a significant volume of gas. Furthermore, the reservoir must not be associated with freshwater aquifers due to the huge importance of this resource for human life (Xu et al. 2004; Lu et al. 2022). Computational models vary in their conclusions but generally indicate that ideal reservoirs are found at depths greater than 800 m, comprising a layer at least 20 m thick and sealed by cap rock at least 10 m thick (Soong et al. 2004; Xu et al. 2005; André et al. 2007; Qu et al. 2022). The Rio Bonito Formation of the Paraná Basin has demonstrated the greatest potential for CCS actions in South America, with packages of porous, quartz, and feldspathic sandstones and thick coal seams and carbonaceous shales with a high organic matter content, which are strategic rocks due to its high CO_2 adsorption capacity (Ketzer et al. 2009; Abraham-A and Tassinari 2023; de Oliveira et al. 2023; Abraham-A et al. 2024a; 2024b).

This study unveils the first finding of natural dawsonite within the Rio Bonito Formation, occurring in quartz sandstones sampled from cores associated with wells drilled for coal exploration along the eighties. The dawsonite identification in this formation improves its potential for mineral trapping (CCS), confirming that the Rio Bonito Formation provides the required conditions for dawsonite crystallization. The characterization of dawsonite, its textures, and associated microstructures was carried out using petrographic microscopy, scanning electron microscopy (SEM) with coupled energy dispersive x-ray spectroscopy (EDX) system and x-ray diffraction (XRD).

Geological background

The Rio Bonito Formation is part of the Gondwana I Supersequence (Carboniferous-Lower Triassic) of the Paraná Basin (Milani et al. 2007). The Rio Bonito Formations is part of the transgressive portion of the Permo-Carboniferous transgressive–regressive cycle recorded in this supersequence. It comprises conglomerate, very fine- to very coarse-grained sandstone, claystone, and coal seams, some of which have economic significance. The Rio Bonito Formation contains significant reserves of methane adsorbed in the coal layers, which are preserved due to adequate sealing (Kalkreuth et al. 2008; 2013). Its deposition is related to tidal-dominated fluvial and estuarine environments and wave-dominated shoreface environments (Perinotto and Castro 2000; Lopes and Lavina 2001; Holz 2003; Cagliari et al. 2014; Bicca et al. 2020; Kern et al. 2021).

The Rio Bonito Formation may be up to 350 m thick, with an average thickness exceeding 170 m. Positioned in the central-southern region of the Paraná Basin, it occurs at a target depth exceeding 800 m, meeting the requirements for CO_2 storage. It is overlain by the Palermo Formation, which serves as a proposed sealing rock, with a minimum thickness of 20 m and an average thickness surpassing 120 m. The Palermo Formation is composed of fine- to very fine-grained sandstones and siltstones interspersed with thinly laminated shales, mudstones, and occasionally limestones (Ramos et al. 2015; de Oliveira et al. 2023; Abraham-A 2023; 2024a). The Rio Bonito Formation thins out towards the south of the basin. In the Rio Grande do Sul State, where dawsonite was found (Fig. 1), the greatest thicknesses of the formation (ranging from 150 to 200 m) are related to paleo valleys distributed along the basin's edge. However, these thicknesses may significantly diminish over the basement highs (Ketzer et al. 2003; Jasper et al. 2006).

The Well 5-CA-91-RS (Fig. 2 and 3) drilled by the Geological Survey of Brazil (SGB-CPRM) provided the study samples. This well cuts into the Pirambóia (Fig. 1), Rio do Rasto and Palermo formations before reaching the Rio Bonito Formation. Dawsonite was identified in quartz sandstones at depths from 541.20 to 541.05 m (Fig. 3A) and

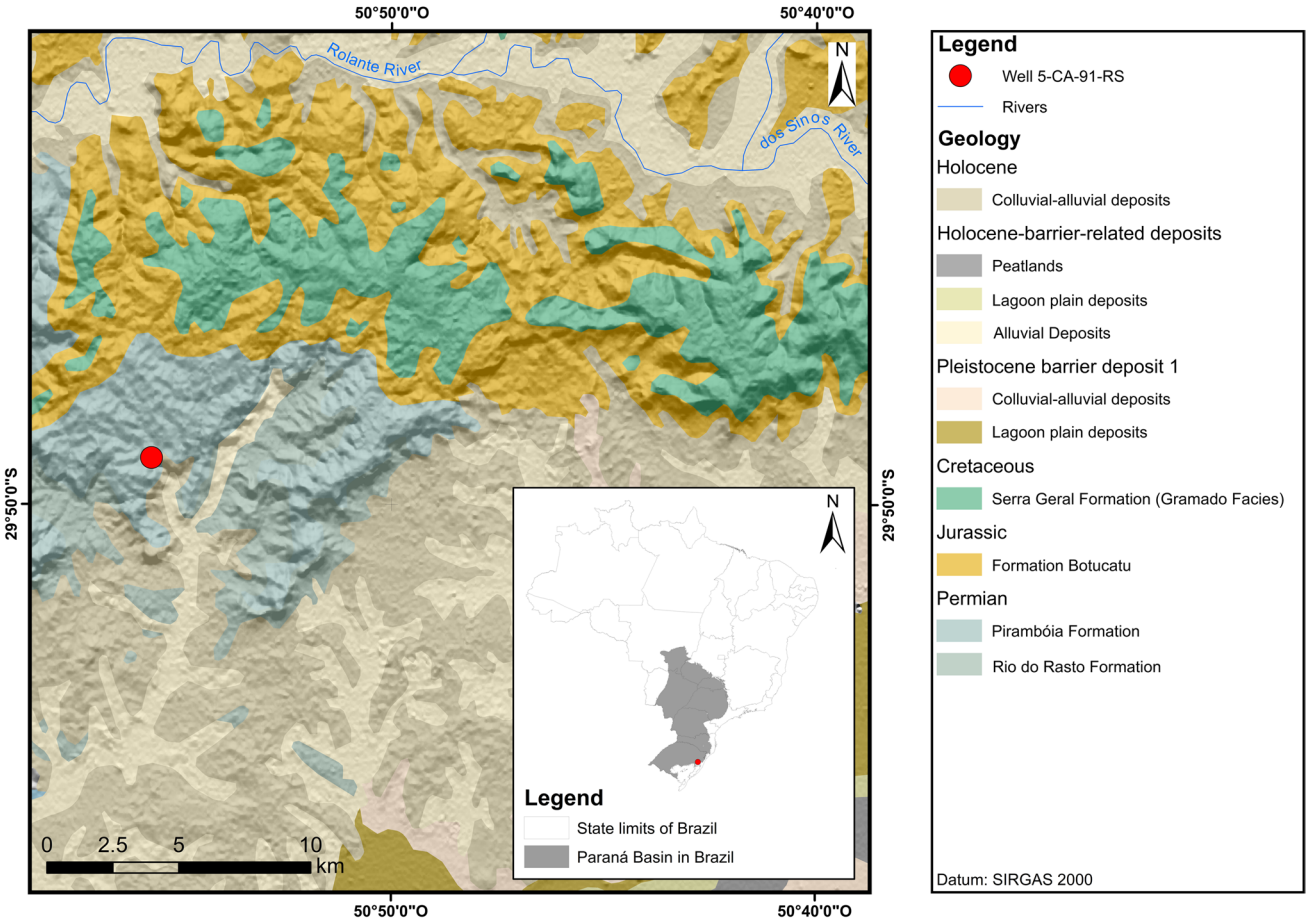

Fig. 1 Geological map of the area where well 5-CA-91-RS was drilled

566.25 to 566.00 m (Fig. 3B), herein referred to as intervals A and B (Fig. 2).

Porosity ranges between 10 and 20% in the sandstones and 1.6 to 4.3% in the coal seams of the Rio Bonito Formation (Milani et al. 2007; Ketzer et al. 2003; Lourenzi and Kalkreuth 2014). In addition to sandstones, coal seams, and carbonaceous shales also have potential for CO_2 adsorption due to their relevant contents of organic matter, ranging from 5 to 25% (Lourenzi and Kalkreuth 2014; Costa et al. 2016; Bicca et al. 2020). De Oliveira et al. (2023) conducted stratigraphic correlations between drilling cores in the Paraná Basin, mapping an area of 383,951 km^2 where the Rio Bonito Formation fully meets the requirements for onshore mineral trapping.

Material and methods

Sample collection and preparation

The studies were conducted on cores from well 5-CA-91-RS (Fig. 3) provided by the Geological Survey of Brazil (SGB-CPRM) and stored at its headquarters in Caçapava do Sul City, in the central portion of the Rio Grande do Sul State. The 4.85 cm wide well was drilled between 1976 and 1977 in the Gravataí municipality as part of a coal exploration campaign promoted by the Brazilian Ministry of Mines and Energy. The rock samples were repurposed in 2023 to evaluate mineral trapping potential. SGB-CPRM provided 2 kg (equivalent to 0.75 L) of rock samples from the Rio Bonito Formation for characterization tests.

A portion of this material was cut into $4 \times 2 \times 0.5$ cm slivers using a cutting disc to prepare thin sections for microscopy following a method adapted from Pike and Kemp (1996) and Adams et al. (2014). The slivers were immersed in a mixture of 10 g of epoxy resin, 0.5 g of Oracet B® blue dye (to dye the rock's porous blue), and 5 g of Araldite® hardening agent dissolved in 50 mL of hydrated ethanol to liquefy the mixture. This solution was then subjected to a vacuum pump for 24 h to ensure complete percolation throughout the porosity of the quartz sandstones. After drying and subsequent resin hardening, the samples were affixed onto a glass slide and polished until they reached a thickness of 30 µm. The choice of

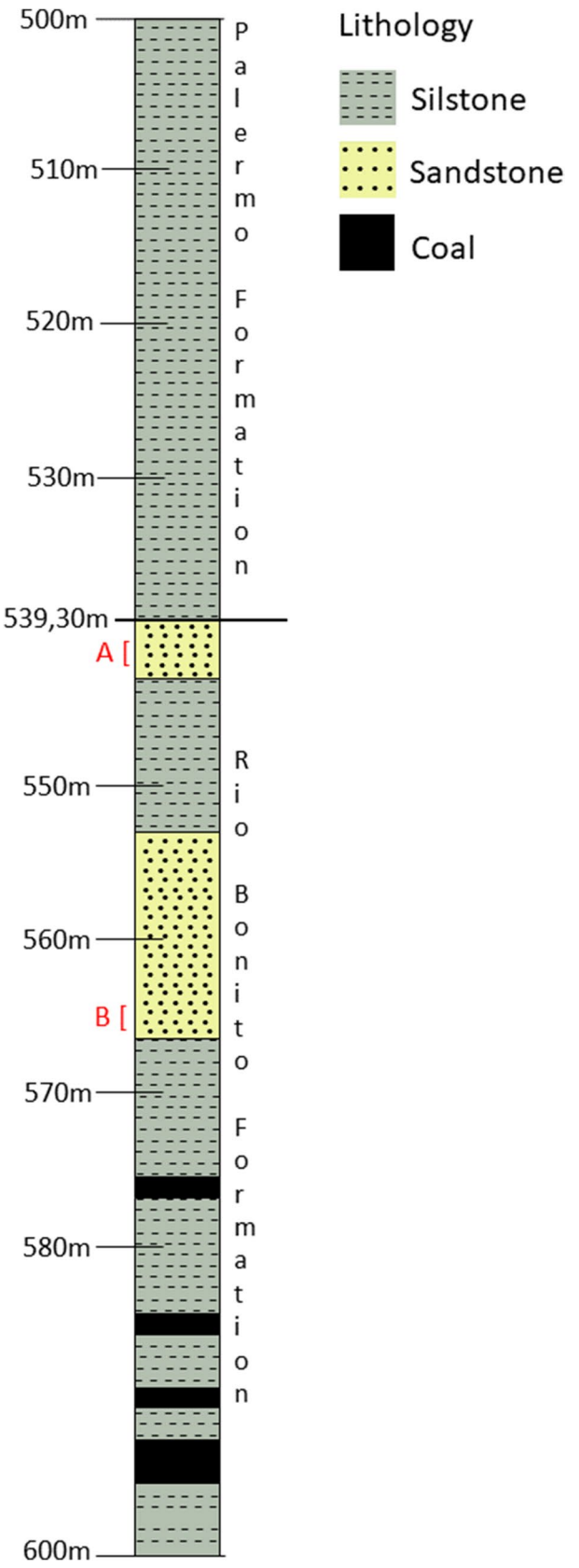

Fig. 2 Stratigraphic sequence of well 5-CA-91-RS between 500 and 600 m depth, showing the Palermo and Rio Bonito Formations. **A** and **B** represent the dawsonite finding zones. **A** between 541.20 and 541.05 m, and **B** between 566.25 and 566.00 m

resins was an adaptation of traditional methods to optimize costs and sample preparation time, as observed in adaptations to other sedimentary materials (see Montana 2020; Broekmans et al. 2022). The same thin sections used in petrography were utilized for SEM–EDX analysis. Thin sections for microscopy were prepared at the Geological Thin Section Laboratory of the Universidade do Vale do Rio dos Sinos (UNISINOS).

For XRD analysis, 1 kg of sample was ground to 75 µm (#200 mesh) followed by successive homogenization stages and quartering until 10 g of powder was selected. Given the homogeneous nature of the quartz sandstone, no special care was required to select any specific rock segment for grinding, in accordance with the methods of Waseda et al. (2011) and Ali et al. (2022).

Analytical methods

Petrographic analyses were conducted using a Zeiss AxioLab A1 Microscope with a Zeiss AxioCam MRc camera system from the Fluid Inclusion Lab at UNISINOS.

SEM–EDX analyses were performed at the Technological Institute of Paleoceanography and Climate Change (ITT OCEANEON) at UNISINOS in Zeiss EVO MA 15 electron microscope. The microscope operated at an acceleration voltage (EHT) of 25 kV and a working distance (WD) of 8.5 mm, with a probe current of 8 nA. Samples were gold-coated with a layer thickness of 46 nm. The SEM was coupled with an Oxford Instruments EDX spectrograph featuring an X-Max detector. Analyses were performed over seven interactions with a live time of 180 s each. This analytical technique was employed to generate false-color images for mapping strategic chemical elements (C, O, Na, Al, and Si) to identify dawsonite in quartz sandstone, following the methodology outlined by Gomes (2015).

XRD was performed at ITT OCEANEON at UNISINOS on an Empyrean PANalytical diffractometer with a reflection-transmission configuration, spinning at two revolutions per second, with a goniometric range from 2 to 75° (2θ), a step of 0.0131° with 170 s per step, and a Cu tube operating at 40 kV and 40 mA. Bragg–Brentano HD incident beam geometry was used, with a 0.02 rad Soller slit, a 20 mm fixed mask, a 1/4" fixed anti-scattering slit, and a 1/16" fixed divergent slit. A 7.5 mm anti-scattering slit and a 0.02 rad

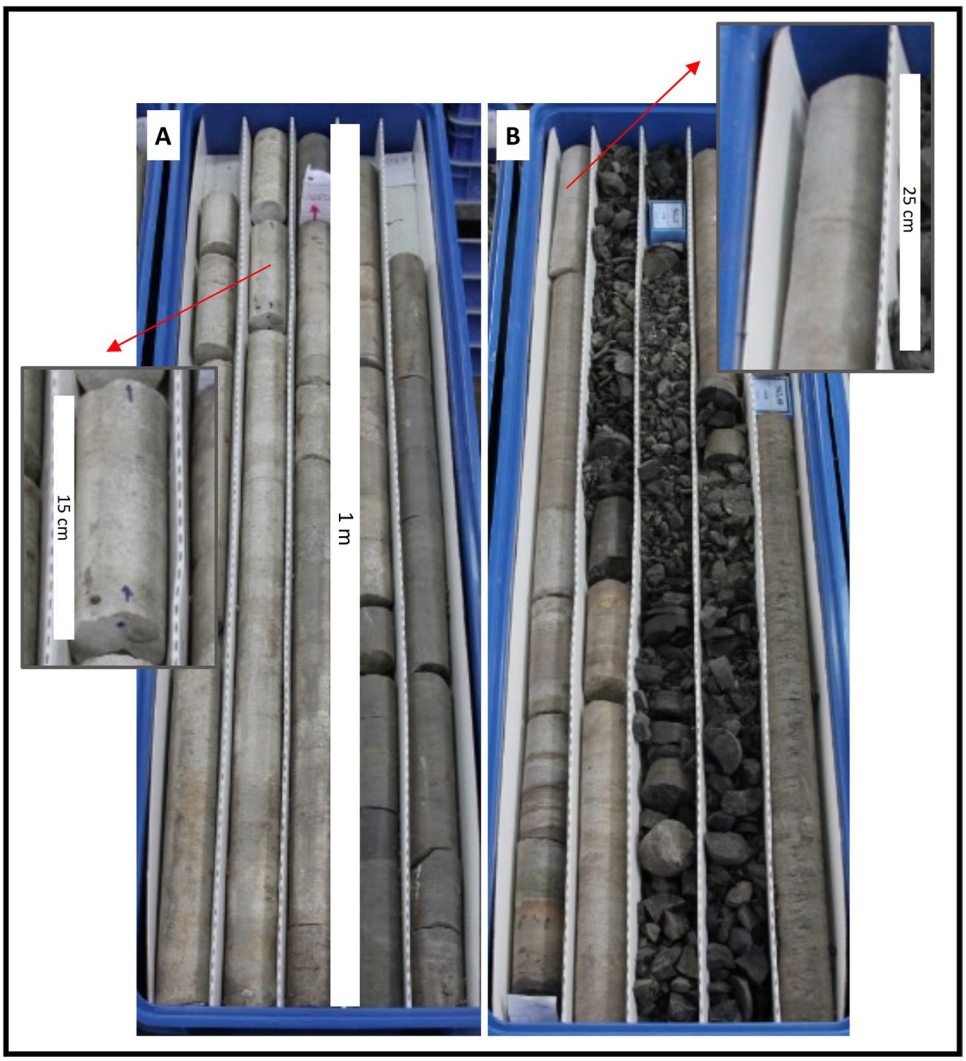

Fig. 3 Cores from well 5-CA-91-RS. **A** Core from 541.20 and 541.05 m and **B** core from 566.25 to 566.00 m. Both intervals (**A** and **B**) contain dawsonite

Soller slit were mounted on the diffracted beam. The diffractometer was equipped with a PIXcel 3DMedipix3 area detector with 255 channels.

Results

Dawsonite (Fig. 4B, 4C and 4E) was initially found in thin sections under polarized light optical microscopy (petrographic microscopy) within quartz sandstones containing grains ranging from 0.2 mm to 1.5 mm (Fig. 4A), alongside carbonate (identified in XRD as dolomite) and muscovite. The sandstone exhibited moderate to well-sorting, with subangular to subrounded grains. Two types of pores, measuring 0.1 to 1.0 mm, were observed: isolated intergranular primary porosity (Fig. 4D) and moldic secondary porosity (Fig. 4G), indicating mineral dissolution during diagenesis. Diagenetic processes include quartz overgrowth (Fig. 4F), carbonate cement deposition (Fig. 4H), and partial dissolution of framework grains, formingwhich form moldic pores where dawsonite precipitated during mesodiagenesis (Fig. 4B-G).

Following the identification of dawsonite as thin radiating acicula filling the moldic porosity of the quartz sandstones (Fig. 5A), the sample was analyzed by SEM for compositional imaging using EDX (Fig. 5). In the image captured by secondary and backscattered electrons (respectively Fig. 5A and 5B), the contrast in morphology and average atomic number between the unfilled pore, dawsonite, and quartz-dominated framework is discernible. The simultaneous presence of carbon (Fig. 5C), oxygen (Fig. 5D), sodium (Fig. 5E), and aluminum (Fig. 5F), alongside the complete absence of silicon (Fig. 5G), corroborates the petrographic observations.

Definitive confirmation of the dawsonite occurred after performing an XRD analysis on the total rock powder (Fig. 6). The XRD results confirmed the presence of dawsonite, identified the carbonate as dolomite, and confirmed the presence of muscovite.

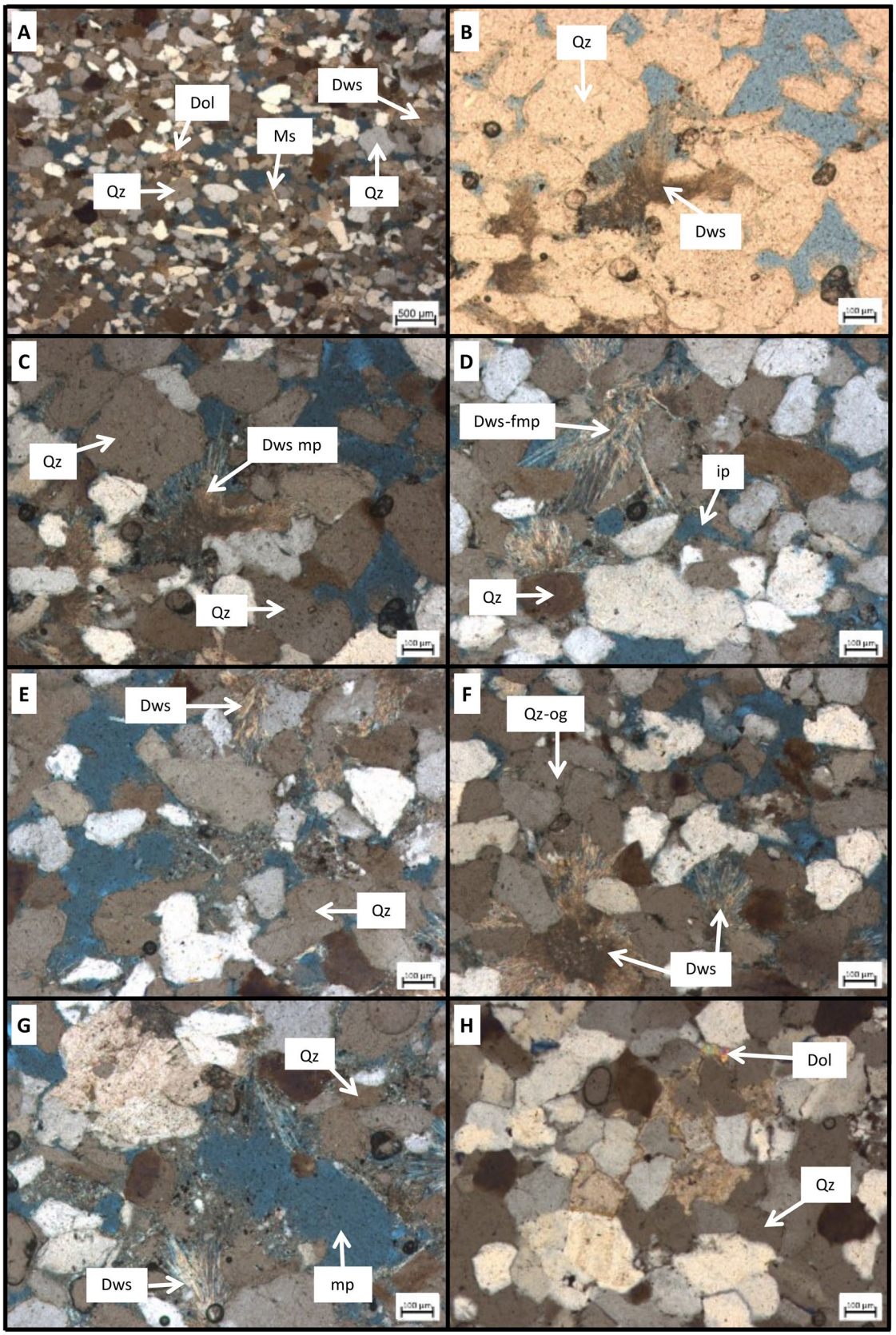
A
Dol
Dws
Ms
Qz
Qz
500 µm
B
Qz
Dws
100 µm
C
Qz
Dws mp
Qz
100 µm
D
Dws-fmp
ip
Qz
100 µm
E
Dws
Qz
100 µm
F
Qz-og
Dws
100 µm
G
Qz
Dws
mp
100 µm
H
Dol
Qz
100 µm

◂**Fig. 4** Thin sections of quartz sandstones of the Rio Bonito Formation in the well 5-CA-91-RS. Photos **A** and **C** to **H** correspond to cross-polarized transmitted-light images and **B** relates to a polarized transmitted-light image. **A** Quartz (Qz) sandstone with dolomite (Dol), muscovite (Ms), and dawsonite (Dws). **B**, **C**, **E**, and **G** show dawsonite formed from moldic porosity (Dws mp). **D** Example of an isolated pore (ip) and dawsonite-filled moldic pore (Dws-fmp). **F** Quartz overgrowth (Qz-og). **H** Carbonate cementation (dolomite) in quartz sandstone. Mineral abbreviations follow Whitney and Evans (2010) for Dol, Ms, and Qz, while the nomenclature for Dws follows Warr (2021)

Final remarks

The literature presents several technological uses for dawsonite, such as in catalysts (Zumbar et al. 2021), fire retardants (Zhang et al. 2024), nanotechnology (Duan et al. 2013), sorbents (Zhao et al. 2020) and water treatment (Li et al. 2020). These applications highlight the dawsonite's potential for advanced applications (Nobre et al. 2022b, 2023). These

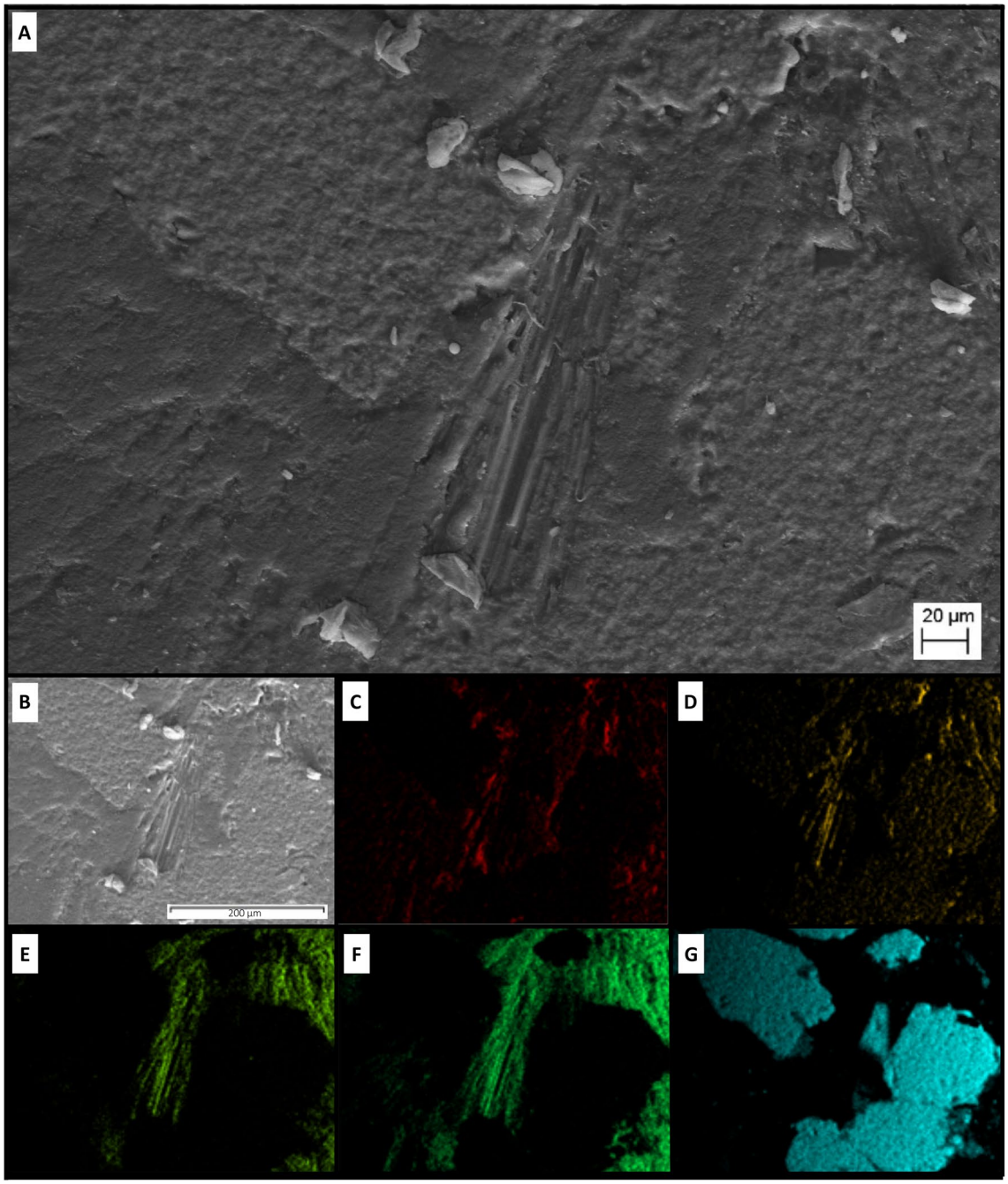

Fig. 5 SEM of dawsonite grown in moldic porous and its surroundings. **C-G** are on the same scale shown in **B**. **A** Secondary electron image. **B** Backscattered electron image. **C** Compositional image of carbon. **D** Compositional image of oxygen. **E**, **F**, and **G** correspond to compositional images of sodium, aluminum, and silicon, respectively

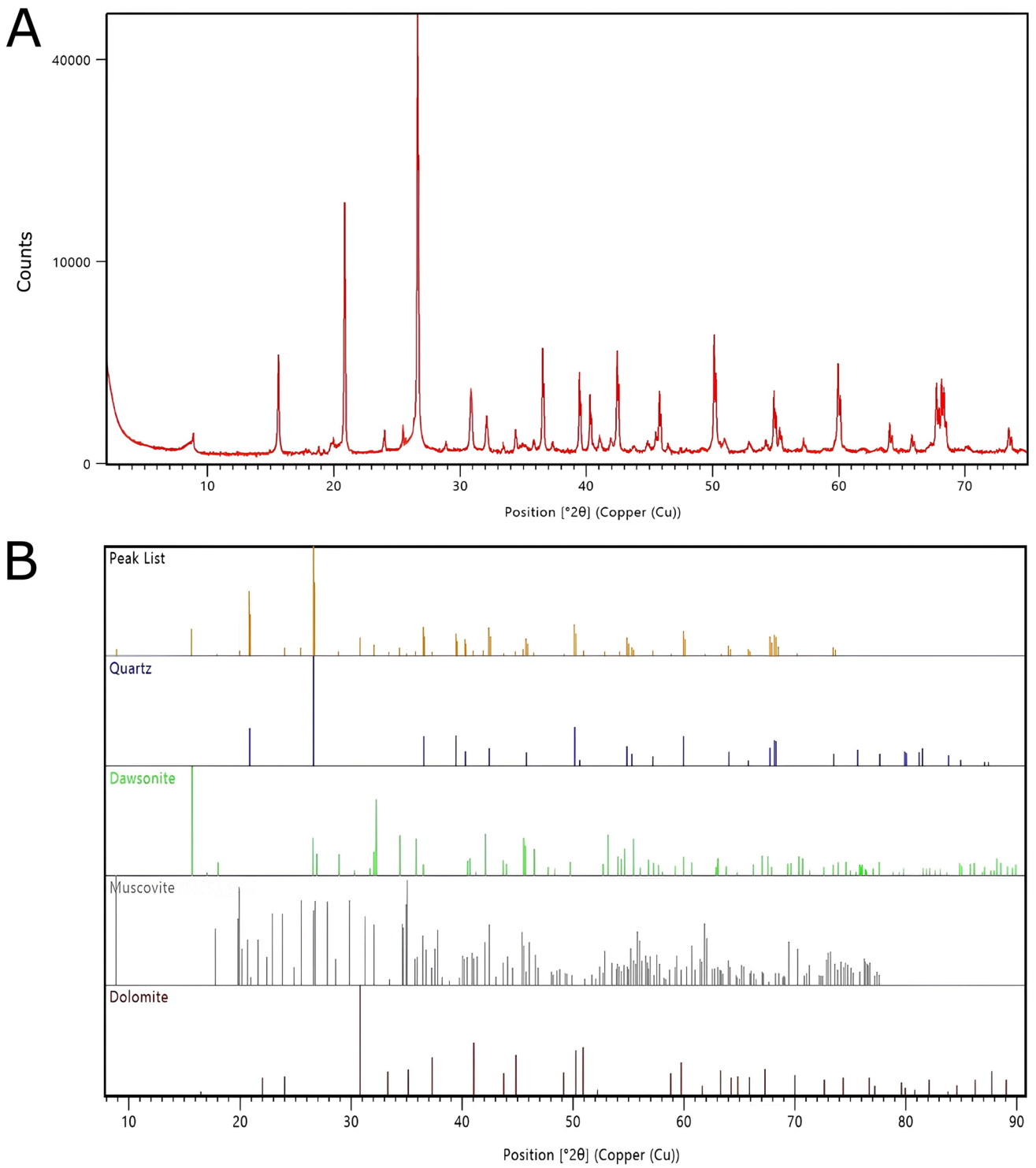

Fig. 6 XRD results of powder from total quartz sandstone sample of the Rio Bonito Formation. **A** The diffractogram of total rock powder. **B** Interpretation of XRD results: Quartz was identified by the main peak at 2θ = 26.5º, and the secondary peak at 2θ = 21º; dawsonite was diagnosed by its main peak at 2θ = 15.5º, and the secondary peak at 2θ = 32º; muscovite was detected by its main peak at 2θ = 9º, and the secondary peak at 2θ = 26.5º; and dolomite was verified by its main peak at 2θ = 31º, and the secondary peak at 2θ = 41º

advanced applications rely on synthetic crystals, as natural dawsonite is not typically abundant or stable enough at the surface to be mined as a commodity. However, its crystallization induced by high pCO_2 levels makes dawsonite prominent as a CCS strategy.

The discovery of dawsonite in the Rio Bonito Formation represents a significant advancement in understanding the potential of this unit for CO_2 trapping, particularly within quartz sandstones as investigated in this study. This paper marks the first documented occurrence of dawsonite within the Rio Bonito Formation. Dawsonite formed during mesodiagenesis and was always found filling moldic pores, indicating that some primary minerals dissolved in earlier diagenetic stages, creating the necessary chemical conditions for dawsonite formation. Thus, the documented dawsonite is not a primary mineral, aligning with descriptions in the literature that highlight its common authigenic occurrence (Saldanha et al. 2023; Cseresznyes et al. 2024).

In the studied region, the Rio Bonito Formation is closer to the surface than in the Paraná Basin depocenter. In this context, dawsonite was found at depths of 541.20 to 541.05 m and 566.25 to 566.00 m. While these depths are shallow for mineral trapping initiatives, they facilitate sample acquisition, as drilling depths exceeding 800 m are substantially more expensive. Previous studies (Ketzer et al. 2009; Abraham-A and Tassinari 2023; de Oliveira et al. 2023; Abraham-A et al. 2024a; 2024b) have demonstrated the high potential of the Rio Bonito Formation for CO_2 storage in the basin's deeper portions. The finding of dawsonite reinforces this potential, as it is the most prominent mineral formed in the CO_2 mineral trapping process. It is reasonable to infer that occurrences of dawsonite may exist in other sections of the Rio Bonito Formation, particularly those adjacent to layers of coal and organic matter-rich shales within the same unit. As a result, the discovery of dawsonite in the Rio Bonito Formation reinforces the potential of the Paraná Basin for onshore storage of considerable volumes of CO_2 in the future.

The petrophysical characteristics of the Rio Bonito Formation such as porosity, depth, thickness, and the presence of an effective sealing layer, highlights its growing potential for future CCS initiatives. Moreover, the presence of natural dawsonite further enhances this potential.

Acknowledgements The authors would like to thank the Brazilian Geological Service (SGB-CPRM) for providing the samples. Special thanks are extended to the Geological Thin Section Laboratory and the Fluid Inclusion Microscopy Laboratory at UNISINOS for their assistance in sample preparation and petrographic microscopy analyses. Additionally, we acknowledge the Technological Institute of Paleoceanography and Climate Change (itt OCEANEON) at UNISINOS for conducting the XRD and SEM-EDX analyses.

References

Abraham-A RM, Tassinari CCG (2023) Carbon dioxide storage efficiency involving the complex reservoir units associated with Irati and Rio Bonito Formations, Paraná Basin, Brazil. AAPG Bull 107:357–386. https://doi.org/10.1306/EG08232121005

Abraham-A RM, Cañas SSM, Miranda IFS, Tassinari CCG (2024a) Assessment of CO_2 storage prospect based on physical properties of Rio Bonito Formation rock units. Energy Geosci 5:100163. https://doi.org/10.1016/j.engeos.2023.100163

Abraham-A RM, Rocha HV, de Oliveira SB, Tassinari CCG, da Silva OC (2024b) Hydrocarbon indication in Rio Bonito Formation sandstone: Implication for CO_2 storage in São Paulo. Brazil Energy Geosci 5:100168. https://doi.org/10.1016/j.engeos.2023.100168

Adams AE, MacKenzie WS, Guilford C (2014) Atlas of sedimentary rocks under the microscope. Routledge Taylor & Francis Group, London, p 104

Ali A, Chiang YW, Santos RM (2022) X-ray Diffraction Techniques for Mineral Characterization: A Review for Engineers of the Fundamentals, Applications, and Research Directions. Minerals 12:205. https://doi.org/10.3390/min12020205

André L, Audigane P, Azaroual M, Menjoz A (2007) Numerical modeling of fluid–rock chemical interactions at the supercritical CO_2–liquid interface during CO_2 injection into a carbonate reservoir, the Dogger aquifer (Paris Basin, France). Energy Convers Manag 48:1782–1797. https://doi.org/10.1016/j.enconman.2007.01.006

Bachu S, Gunter WD, Perkins EH (1994) Aquifer disposal of CO2: Hydrodynamic and mineral trapping. Energy Conversion and Management 35(4):269–279. https://doi.org/10.1016/0196-8904(94)90060-4

Bicca MM, Kalkreuth W, da Silva TF, de Oliveira CHE, Genezini FA (2020) Thermal and depositional history of Early-Permian Rio Bonito Formation of southern Paraná Basin – Brazil. Int J Coal Geol 228:103554. https://doi.org/10.1016/j.coal.2020.103554

Broekmans MATM, Fernandes I, Fredin O, Margreth A (2022) Polarization-fluorescence Microscopy in the Study of Aggregates and Concrete. Elements 18:321–326. https://doi.org/10.2138/gselements.18.5.321

Burnham AK, Levchenko A, Herron MM (2015) Analysis, occurrence, and reactions of dawsonite in AMSO well CH-1. Fuel 144:259–263. https://doi.org/10.1016/j.fuel.2014.12.018

Cagliari J, Lavina ELC, Philipp RP, Tognoli FMW, Basei MAS, Faccini UF (2014) New Sakmarian ages for the Rio Bonito formation (Paraná Basin, southern Brazil) based on LA-ICP-MS U-Pb radiometric dating of zircons crystals. J South Am Earth Sci 56:265–277. https://doi.org/10.1016/j.jsames.2014.09.013

Comerio M, Morosi ME, Tunik M, Paredes JM, Zalba PE (2014) The Role of Telogenetic Injection of Magmatically Derived CO_2 in the Formation of Dawsonite from the Castillo Formation, Chubut Group, Patagonia, Argentina. Can Mineral 52:513–531. https://doi.org/10.3749/canmin.52.3.513

Costa OL, Kionka DCO, Perico E, Jasper A (2016) Identificação de carvão vegetal macroscópico no nível de roof-shale do Afloramento Quitéria, Formação Rio Bonito, permiano inferior da Bacia do Paraná. Geosul 31:133–155. https://doi.org/10.5007/2177-5230.2016v31n61p133

Cseresznyes D, Király C, Gál A, Papucs A, Kónya P, Lakos I, Kovács I, Rinyu L, Szamosfalvi A, Szabó C, Falus G, Czuppon G (2024) Surface occurrence of dawsonite and natural CO2 emanation in Covasna, in the Eastern Carpathians: A stable isotope study. Chem Geol 645:121883. https://doi.org/10.1016/j.chemgeo.2023.121883

De Oliveira SB, Weber N, Yeates C, Tassinari CCG (2023) Geological screening for onshore CO2 storage in the Rio Bonito formation, Paraná Basin. Brazil J Maps 19:2171817. https://doi.org/10.1080/17445647.2023.2171817

Dong LS, Liu L, Meng QA, Zhang G, Wang LJ, Zhao S, Zhou B (2011) Generation of Dawsonite Cement of Pyroclastic Rocks in Tongbomiao Formation in Tanan Sag of Tamtsag Basin in Mongolia. J Jilin Univ 41:421–431. https://doi.org/10.13278/j.cnki.jjuese.2011.02.036

Duan X, Kim T, Han L, Ma J, Du X, Zheng W (2013) Formation of Alumina Nanocapsules by High-Energy-Electron Irradiation of Na-dawsonite Nanorods. Sci Rep 3:3218. https://doi.org/10.1038/srep03218

Gao Y, Liu L, Hu W (2009) Petrology and isotopic geochemistry of dawsonite-bearing sandstones in Hailaer basin, northeastern China. Appl Geochem 24:1724–1738. https://doi.org/10.1016/j.apgeochem.2009.05.002

Gaus I, Azaroual M, Czernichowski-Lauriol I (2005) Reactive transport modelling of the impact of CO2 injection on the clayey cap rock at Sleipner (North Sea). Chem Geol 217:319–337. https://doi.org/10.1016/j.chemgeo.2004.12.016

Golab AN, Carr PF, Palamara DR (2006) Influence of localised igneous activity on cleat dawsonite formation in Late Permian coal measures, Upper Hunter Valley Australia. Int J Coal Geol 66(4):296–304

Goldbery R, Loughnan FC (1977) Dawsonite, alumohydrocalcite, nordstrandite and gorceixite in Permian marine strata of the Sydney Basin, Australia. Sedimentology 24:565–579. https://doi.org/10.1111/j.1365-3091.1977.tb00139.x

Gomes CB (2015) A microssonda eletrônica na geologia. São Paulo: EDUSP. https://repositorio.usp.br/directbitstream/a561df7b-a05e-4eb6-8a31-c756de11874d/2681553_compressed.pdf

Harrington BJ (1875) Notes on dawsonite, a new carbonate. Can Nat and Quat. J of Sci 7:305–309

Hay RL, Reeder RJ (1991) Calcretes of Olduvai Gorge and the Ndolanya Beds of Northern Tanzania. Calcretes 25:649–673. https://doi.org/10.1002/9781444304497.ch1

Hellevang H, Aagaard P, Oelkers EH, Kvamme B (2005) Can Dawsonite Permanently Trap CO_2? Environ Sci Technol 39:8281–8287. https://doi.org/10.1021/es0504791

Hellevang H, Declercq J, Kvamme B, Aagaard P (2010) The dissolution rates of dawsonite at pH 0.9 to 5 and temperatures of 22, 60 and 77 °C. Appl Geochem 25:1575–1586. https://doi.org/10.1016/j.apgeochem.2010.08.007

Hellevang H, Declercq J, Aagaard P (2011) Why is Dawsonite Absent in CO2 Charged Reservoirs? Oil Gas Sci Technol 66:119–135. https://doi.org/10.2516/ogst/2011002

Hellevang H, Aagaard P, Jahren J (2013) Will dawsonite form during CO2 storage? Greenh Gases: Sci Technol 4:191–199. https://doi.org/10.1002/ghg.1378

Holz M (2003) Sequence stratigraphy of a lagoonal estuarine system—an example from the lower Permian Rio Bonito Formation, Paraná Basin, Brazil. Sediment Geol 162:305–331. https://doi.org/10.1016/S0037-0738(03)00156-8

Jasper A, Menegat R, Guerra-Sommer M, Cazzulo-Klepzig M, Souza PA (2006) Depositional cyclicity and paleoecological variability in an outcrop of Rio Bonito formation, Early Permian, Paraná Basin, Rio Grande do Sul, Brazil. J South Am Earth Sci 21:276–293. https://doi.org/10.1016/j.jsames.2006.05.002

Johnson JW, Nitao JJ, Knauss KG (2004) Reactive transport modelling of CO2 storage in saline aquifers to elucidate fundamental processes, trapping mechanisms and sequestration partitioning. Geol Soc Spec Publ 233:107–128. https://doi.org/10.1144/GSL.SP.2004.233.01.08

Kalkreuth W, Holz M, Casagrande J, Cruz R, Oliveira T, Kern M, Levandowski J, Rolim S (2008) O Potencial de Coalbed Methane (CBM) na jazida da Santa Terezinha – modelagem 3D e avaliação do poço de exploração CBM001-ST-RS. Rev Bras Geo 38(2):3–17

Kalkreuth W, Holz M, Levandowski J, Kern M, Casagrande J, Weniger P, Krooss B The Coalbed Methane (CBM) Potential and CO2 Storage Capacity of the Santa Terezinha Coalfield, Paraná Basin, Brazil – 3D Modelling, and Coal and Carbonaceous Shale Characteristics and Related Desorption and Adsorption Capacities in Samples from Exploration Borehole CBM001-ST-RS. Energ Explor Exploit 31(4): 485-527. https://doi.org/10.1260/0144-5987.31.4.485

Kaszuba JP, Viswanathan HS, Carey JW (2011) Relative stability and significance of dawsonite and aluminum minerals in geologic carbon sequestration. Geophys Res Lett 38:L08404. https://doi.org/10.1029/2011GL046845

Kern HP, Lavina ELC, Paim PSG, Girelli TJ, Lana C (2021) Paleogeographic evolution of the southern Paraná Basin during the Late Permian and its relation to the Gondwanides. Sediment Geol 415:105808. https://doi.org/10.1016/j.sedgeo.2020.105808

Ketzer JM, Holz M, Al-Aasm MIS (2003) Sequence stratigraphic distribution of diagenetic alterations in coal-bearing, paralic sandstones: evidence from the Rio Bonito Formation (early Permian), southern Brazil. Sedimentology 50:855–877. https://doi.org/10.1046/j.1365-3091.2003.00586.x

Ketzer JM, Carpentier B, Le Gallo Y, Le Thiez P (2005) Geological Sequestration of CO_2 in Mature Hydrocarbon Fields. Basin and Reservoir Numerical Modelling of the Forties Field. North Sea Oil Gas Sci Technol 60:259–273. https://doi.org/10.2516/ogst:2005016

Ketzer JM, Iglesias R, Einloft S, Dullius J, Ligabue R, de Lima V (2009) Water–rock–CO2 interactions in saline aquifers aimed for carbon dioxide storage: Experimental and numerical modeling studies of the Rio Bonito Formation (Permian), southern Brazil. J Appl Geochem 24:760–767. https://doi.org/10.1016/j.apgeochem.2009.01.001

Knorpp AJ, Allegri P, Huangfu S, Vogel A, Stuer M (2023) Synthesis and Characterization of High-Entropy Dawsonite-Type Structures. Inorg Chem 62:4999–5007. https://doi.org/10.1021/acs.inorgchem.3c00179

Li F, Li W (2016) Controlling factors for dawsonite diagenesis: a case study of the Binnan Region in Dongying Sag, Bohai Bay Basin, China. Aust J Earth Sci 63:217–233. https://doi.org/10.1080/08120099.2016.1173096

Li F, Cao Y, Li W, Zhang L (2017) CO_2 mineral trapping: Hydrothermal experimental assessments on the thermodynamic stability of dawsonite at 4.3 Mpa pCO_2 and elevated temperatures. Greenh Gases: Sci Technol 8:77–92. https://doi.org/10.1002/ghg.1699

Li B, Zheng JQ, Guo JZ, Dai CQ (2020) A novel route to synthesize MOFs-derived mesoporous dawsonite and application in elimination of Cu(II) from wastewater. Chem Eng J 383:123174. https://doi.org/10.1016/j.cej.2019.123174

Li F, Diao H, Ma W, Wang M (2022) Study of corrosion mechanism of dawsonite led by CO2 partial pressure. Front Earth Sc 16:465–482. https://doi.org/10.1007/s11707-021-0901-1

Li F, Zhang C, Wang K, Ma W, Yang J, Du Q, Deng S, Liu K (2023) The influence of CO2 partial pressure on the stability of dawsonite-based on water-rock physical experiment and numerical simulation. Appl Geochem 153:105669. https://doi.org/10.1016/j.apgeochem.2023.105669

Li F, Ma W, Zhang C, Wang K (2024) Evolution of Diagenetic Fluid of the Dawsonite-Bearing Sandstone in the Jiyang Depression, Eastern China. J Ocean Univ China 23:80–98. https://doi.org/10.1007/s11802-024-5501-8

Limantseva OA, Makhnach AA, Ryzhenko BN, Cherkasova EV (2008) Formation of Dawsonite Mineralization at the Zaozernyi Deposit,

Belarus. Geochem Int 46:62–76. https://doi.org/10.1134/S0016702908010059

Liu N, Liu L, Qu X, Yang H, Wang L, Zhao S (2011) Genesis of authigene carbonate minerals in the Upper Cretaceous reservoir, Honggang Anticline, Songliao Basin: A natural analog for mineral trapping of natural CO_2 storage. Sediment Geol 237:166–178. https://doi.org/10.1016/j.sedgeo.2011.02.012

Lohuis JAO (1993) Carbon dioxide disposal and sustainable development in the Netherlands. Energy Convers Manag 34:815–821. https://doi.org/10.1016/0196-8904(93)90024-5

Lopes RDC, Lavina ELC (2001) Estratigrafia de sequências nas Formações Rio Bonito e Palermo (Bacia do Paraná), na região carbonífera do Jacuí, Rio Grande do Sul. In: Ribeiro HJP (ed) Estratigrafia de Sequências: Fundamentos e aplicações. Editora Unisinos, São Leopoldo, pp 391–419. https://edunisinos.com.br/produto/17/estratigrafia-de-seq%C3%BCencias-fundamentos-e-aplicacoes

Loughnan FC, Goldbery R (1972) Dawsonite and Analcite in the Singleton Coal Measures of the Sydney Basin. Am Min 57:1437–1447

Lourenzi PS, Kalkreuth W (2014) O potencial de geração CBM (Coalbed Methane) na jazida Sul Catarinense: 1. Características petrográficas e químicas das camadas de carvão da Formação Rio Bonito, Permiano da Bacia do Paraná. Braz J Geol 44:471–491. https://doi.org/10.5327/Z2317-4889201400030009

Lu P, Zhang G, Huang Y, Apps J, Zhu C (2022) Dawsonite as a Temporary but Effective Sink for Geological Carbon Storage. Int J Greenh Gas Control 119:103733. https://doi.org/10.1016/j.ijggc.2022.103733

Marinos D, Kotsanis D, Alexandri A, Balomenos E, Panias D (2021) Carbonation of Sodium Aluminate/Sodium Carbonate Solutions for Precipitation of Alumina Hydrates—Avoiding Dawsonite Formation. Crystals 11:836. https://doi.org/10.3390/cryst11070836

Milani JE, Melo JH, de Souza PA, de Fernandes LA, França AB (2007) Bacia Do Paraná b Geoci Petrobras 15:265–287

Ming XR, Liu L, Yu L, Bai HG, Yu ZC, Liu N, Yang HX, Wang FG, Li BX (2017) Thin-film dawsonite in Jurassic coal measure strata of the Yaojie coalfield, Minhe Basin, China: A natural analogue for mineral carbon storage in wet supercritical CO_2. Int J Coal Geol 180:83–99. https://doi.org/10.1016/j.coal.2017.07.007

Montana G (2020) Ceramic raw materials: how to recognize them and locate the supply basins—mineralogy, petrography. Archaeol Anthrop Sci 12:175. https://doi.org/10.1007/s12520-020-01130-1

Moore J, Adams M, Allis R, Lutz S, Rauzi S (2005) Mineralogical and geochemical consequences of the long-term presence of CO_2 in natural reservoirs: An example from the Springerville–St. Johns Field, Arizona, and New Mexico, U.S.A. Chem Geol 217:365–385. https://doi.org/10.1016/j.chemgeo.2004.12.019

Nobre AG, Salazar-Naranjo AF, Andrade FRD, Vlach SRF, Ando RA (2022b) Simulation of geological graphene genesis by the piston-cylinder apparatus. Matéria (rio J) 27(4):e20220122. https://doi.org/10.1590/1517-7076-RMAT-2022-0122

Nobre AG, Andrade FRD, Salazar-Naranjo AF, Rigue JN, da Silva RB, Vlach SRF, Ando RA (2023) Electrical Resistance Evolution of Graphite and Talc Geological Heterostructures under Progressive Metamorphism. C 9(3):75

Nobre AG, Martínez JAE, Florêncio O (2021) Mineral Nanotechnology in Circular Economy. In: Iano Y, Saotome O, Kemper G, Mendes de Seixas AC, Gomes de Oliveira, G (eds) Smart Innovation, Systems and Technologies, vol 233. Springer, Cham, pp 220–226. https://doi.org/10.1007/978-3-030-75680-2_26

Nobre AG, da Silva LPN, Andrade, FRD (2022a) Graphene Geology and the Fourth Industrial Revolution. In: Iano Y, Saotome O, Kemper Vásquez GL, Cotrim Pezzuto C, Arthur R, Gomes de Oliveira G. (eds) Smart Innovation, Systems and Technologies, vol 207. Springer, Cham, pp 342–348. https://doi.org/10.1007/978-3-031-04435-9_34

Okuyama Y (2014) Dawsonite-bearing Carbonate Veins in the Cretaceous Izumi Group, SW Japan: A Possible Natural Analogue of Fracture Formation and Self-sealing in CO2 Geological Storage. Energy Procedia 63:5530–5537. https://doi.org/10.1016/j.egypro.2014.11.586

Palayangoda SS, Nguyen QP (2015) Thermal behavior of raw oil shale and its components. Oil Shale 32:160–171. https://doi.org/10.3176/oil.2015.2.06

Perinotto JAJ, Castro JC (2000) Stratigraphic framework of Rio do Sul and Rio Bonito (Triunfo Member) formations in the Hercílio river valley (SC), Paraná basin (Early Permian). An Acad Bras Ciênc 72:598–599. https://doi.org/10.1590/S0001-37652000000400013

Pike J, Kemp AES (1996) Preparation and analysis techniques for studies of laminated sediments. Geol Soc Spec Publ 116:37–48. https://doi.org/10.1144/GSL.SP.1996.116.01.05

Qu X, Zhang Y, Li Q, Du T, Li Y (2022) Geological features and occurrence conditions of dawsonite as a main Carbon-Fixing mineral. Alex Eng J 61:2997–3011. https://doi.org/10.1016/j.aej.2021.08.022

Ramos AS, Rodrigues LF, Araujo GE, Pozocco CTM, Ketzer JMM, Heemann R, Lourega RV (2015) Geochemical Characterization of Irati And Palermo Formations (Paraná Basin-Southern Brazil) for Shale Oil/Gas Exploration. Energy Technol 3:481–487. https://doi.org/10.1002/ente.201402107

Reynolds JG, Cooke GA, Herting DL, Wade-Warrant R (2012) Evidence for dawsonite in Hanford high-level nuclear waste tanks. J Hazard Mater 209:186–192. https://doi.org/10.1016/j.jhazmat.2012.01.018

Rybak-Ostrowska B, Gasinski A, Kapron G (2020) Dawsonite as an indicator of multistage deformation and fluid pathways within fault zones: Insights from the Fore-Dukla Thrust Sheet, Outer Carpathians, Poland. Acta Geol Pol 70:51–78. https://doi.org/10.24425/agp.2019.126453

Saldanha JP, Cagliari J, Horodyski RC, Del Mouro L, Pacheco MLAF (2023) Deciphering the origin of dubiofossils from the Pennsylvanian of the Paraná Basin, Brazil. Biogeosciences 20:3943–3979. https://doi.org/10.5194/bg-20-3943-2023

Sirbescu MLC, Nabelek PI (2003) Dawsonite: An inclusion mineral in quartz from the Tin Mountain pegmatite, Black Hills, South Dakota. Am Min 88:1055–1059. https://doi.org/10.2138/am-2003-0714

Soong Y, Goodman AL, McCarthy JR, Baltrus JP (2004) Experimental and simulation studies on mineral trapping of CO_2 with brine. Energy Convers Manag 45:1845–1859. https://doi.org/10.1016/j.enconman.2003.09.029

Teles LSB, Campos JEG, Ramos TG (2022) Light on the origin of the verdete siltstone, Bambuí group, central Minas Gerais state. Brazil J South Am Earth Sci 119:103938. https://doi.org/10.1016/j.jsames.2022.103938

Warr LN (2021) IMA–CNMNC approved mineral symbols. Mineral Mag 85:291–320. https://doi.org/10.1180/mgm.2021.43

Waseda Y, Matsubara E, Shinoda K (2011) X-Ray Diffraction Crystallography Introduction, Examples and Solved Problems. Springer-Verlag, Berlin, 310 pp. https://doi.org/10.1007/978-3-642-16635-8

Whitney DL, Evans BW (2010) Abbreviations for names of rock-forming minerals. Am Min 95:185–187. https://doi.org/10.2138/am.2010.3371

Wopfner H, Höcker CFW (1987) The permian groeden sandstone between bozen and meran (northern Italy), a habitat of dawsonite and nordstrandite. Neues Jahrb Geol Palaontol Abh 3:161–176. https://doi.org/10.1127/njgpm/1987/1987/161

Worden RH (2006) Dawsonite cement in the Triassic Lam Formation, Shabwa Basin, Yemen: A natural analogue for a potential mineral product of subsurface CO2 storage for greenhouse gas reduction. Mar Pet Geol 23:61–77. https://doi.org/10.1016/j.marpetgeo.2005.07.001

Xu T, Apps JA, Pruess K (2004) Numerical simulation of CO_2 disposal by mineral trapping in deep aquifers. J Appl Geochem 19:917–936. https://doi.org/10.1016/j.apgeochem.2003.11.003

Xu T, Apps JA, Pruess K (2005) Mineral sequestration of carbon dioxide in a sandstone–shale system. Chem Geol 217:295–318. https://doi.org/10.1016/j.chemgeo.2004.12.015

Zalba PE, Conconi MS, Morosi M, Manassero M, Comerio M (2011) Dawsonite in tuffs and litharenites of the Cerro Castaño Member, Cerro Barcino Formation, Chubut Group (Cenomanian), Los Altares, Patagonia, Argentina. Can Mineral 49:503–520. https://doi.org/10.3749/canmin.49.2.503

Zhang Y, Wang Z, Li Q, Pan R, Zhou X (2024) A novel approach for enhancing fire suppression efficiency of dry powder extinguishant: From the synergistic effect of dawsonite. Powder Technol 431:119052. https://doi.org/10.1016/j.powtec.2023.119052

Zhao Z, Wang R, Peng X, Deng P, Tian Y, Liu Z, Shi P, Wu L, Zhang Z, Chen C, Liu C (2020) Preparation of pseudo-boehmite through the dawsonite as an intermediate. Inorg Nano-Met Chem 50:1094–1102. https://doi.org/10.1080/24701556.2020.1735425

Zumbar T, Ristic A, Drazic G, Lazarova H, Volavsek J, Pintar A, Logar NZ, Tusar NN (2021) Influence of Alumina Precursor Properties on Cu-Fe Alumina Supported Catalysts for Total Toluene Oxidation as a Model Volatile Organic Air Pollutant. Catal 11:252. https://doi.org/10.3390/catal11020252